

SUPERSOFT X-RAY SOURCES IN M31. II. *ROSAT*-DETECTED SUPERSOFT SOURCES IN THE *ROSAT*, *CHANDRA*, AND *XMM-NEWTON* ERAS

J. GREINER

Max-Planck-Institut für Extraterrestrische Physik, Giessenbachstrasse, 85748 Garching, Germany; jcg@mpe.mpg.de

AND

R. DI STEFANO,¹ A. KONG, AND F. PRIMINI

Harvard-Smithsonian Center for Astrophysics, 60 Garden Street, Cambridge, MA 02138

Received 2003 October 15; accepted 2004 March 22

ABSTRACT

We have performed *Chandra* observations during the past three years of five of the M31 supersoft X-ray sources discovered with *ROSAT*. Surprisingly, only one of these sources has been detected, despite a predicted detection of about 20–80 counts for these sources. This has motivated a thorough check of the *ROSAT* M31 Survey I data, including a relaxation of the hardness ratio requirement used to select supersoft sources. This increases the number of supersoft sources identified in Survey I by seven. We then carried out a comparison with the *ROSAT* M31 Survey II data set, which had hitherto not been explicitly investigated for supersoft X-ray sources. We find that most of the *ROSAT* Survey I sources are not detected, and only two new supersoft sources are identified. The low detection rate in the *ROSAT* Survey II and our *Chandra* observations imply that the variability timescale of supersoft sources is a few months. If the majority of these sources are close binary supersoft sources with shell hydrogen burning, it further implies that half of these sources predominantly experience large mass transfer rates.

Subject headings: binaries: close — galaxies: individual (M31) — novae, cataclysmic variables — X-rays: stars

1. INTRODUCTION

Observations during the past decade have suggested the definition of a new class of sources. Luminous supersoft X-ray sources (SSSs) have luminosities in the range 10^{35} – 10^{38} ergs s^{-1} and kT in the range 20–80 eV, with no hard X-ray component of comparable luminosity. Some SSSs are simply hot white dwarfs (e.g., postnovae) or pre-white dwarfs (in planetary nebulae). What is most intriguing about SSSs, however, is the fact that the physical nature of a majority of the sources with optical identifications is not yet understood. These more mysterious sources include the prototypes CAL 83 and CAL 87, discovered with *Einstein* (Long et al. 1981), and the more numerous examples discovered with *ROSAT* (e.g., Greiner 2000). The most promising explanation for the majority of the sources invokes quasi-steady nuclear burning of matter accreting onto the surface of a white dwarf (WD) to generate these systems' prodigious fluxes (see, e.g., van den Heuvel et al. 1992). There is indirect evidence in favor of these models for several of the sources. The binary sources that are so luminous that nuclear-burning models seem to be required are referred to as close binary supersoft sources (CBSSs).

Observing SSSs in M31 has the advantage that several questions can be attacked more easily than with local sources (including those in the Magellanic Clouds): (1) What is the spatial distribution over the galaxy, and what are the possible correlations with different environments? (2) What is the size of the population, including the ratio of SSSs to other types of low-mass X-ray binaries? (3) What are the variability pattern (if any) and duty cycle? Investigating all these questions can help in providing clues to the nature of the sources.

ROSAT has observed the full disk of the M31 galaxy (about 6.5 deg^2) twice. A *ROSAT* PSPC mosaic of six contiguous pointings with an exposure time of 25 ks each was performed in 1991 July (Survey I; Supper et al. 1997). A second survey was made in 1992 July–August and 1993 January (Survey II; Supper et al. 2001). Until now, only the first survey has been investigated systematically for SSSs (Greiner et al. 1996b).

This paper is the second in a series dealing with SSSs in M31, and in particular with their variability properties. The first (Di Stefano et al. 2004, hereafter Paper I) concentrated on the analysis of several sets of *Chandra* data: (1) three separate 15 ks observations of each of three disk fields and (2) a 40 ks ACIS observation of the bulge with the back side–illuminated (BI) chips, combined with information gleaned from two years of regular ACIS front side–illuminated (FI) chips, monitoring of the bulge. In fact, the disk fields were observed such that the locations of five *ROSAT* SSSs (2, 3, 12, 19, and 20) were covered by the BI chips, which exhibit enhanced sensitivity for very soft X-rays. Another four SSSs (1, 14, 24, and 25) are covered by chance coincidence with the FI chips because of the field rotation between the different epochs. The results of that paper relevant to this second paper can be summarized as follows:

1. That paper established that only one of the *ROSAT*-discovered sources, RX J0038.6+4020, was detected by *Chandra*.
2. No new SSS obeying the same criteria as those applied for the selection in *ROSAT* data has been found in any of these *Chandra* pointings. However, with a modified hardness ratio criterion, a total of 16 new SSSs that are not associated with foreground or background objects, and are therefore likely members of M31, were discovered in the disk fields. Not all of these 16 were luminous enough to have been detected by *ROSAT*; six provided fewer than 20 counts. Furthermore, some

¹ Also Department of Physics and Astronomy, Tufts University, Medford, MA 02155.

TABLE 1
NEW SSSs FROM THE *ROSAT* PSPC

| Number | Name | Coordinates (J2000.0) | Error (arcsec) | Count Rate (counts ks ⁻¹) | HR1 | HR2 |
|---|-----------------|--------------------------|-------------------|--|--------------|--------------|
| First Observation during PSPC Survey I | | | | | | |
| 4..... | RX J0039.3+4047 | 00 39 21.4, +40 47 41 | 42 | 0.26 ± 0.23 | -0.89 ± 0.10 | -0.29 ± 0.65 |
| 6..... | RX J0039.7+4030 | 00 39 47.1, +40 30 05 | 15 | 2.03 ± 0.30 | -0.85 ± 0.10 | -0.83 ± 0.53 |
| 7..... | RX J0039.8+4053 | 00 39 50.4, +40 53 38 | 23 | 1.07 ± 0.25 | -0.75 ± 0.18 | 0.44 ± 0.97 |
| 9..... | RX J0040.4+4013 | 00 40 28.6, +40 13 44 | 23 | 0.50 ± 0.27 | -0.85 ± 0.14 | 0.72 ± 1.00 |
| 14..... | RX J0042.7+4107 | 00 42 44.9, +41 07 18 | 22 | 1.04 ± 0.31 | -0.89 ± 0.16 | -0.65 ± 1.00 |
| 17..... | RX J0044.2+4117 | 00 44 14.0, +41 17 57 | 34 | 0.95 ± 0.35 | -0.97 ± 0.25 | -0.58 ± 0.53 |
| 23..... | RX J0047.6+4159 | 00 47 42.3, +41 59 59 | 36 | 1.23 ± 0.44 | -0.82 ± 0.28 | -0.20 ± 1.00 |
| First Observation during Serendipitous Pointing | | | | | | |
| 21..... | RX J0047.4+4157 | 00 47 27.2, +41 57 34 | 25 | 0.60 ± 0.18 | -0.98 ± 0.21 | 0.00 ± 0.30 |

NOTE.—Units of right ascension are hours, minutes, and seconds, and units of declination are degrees, arcminutes, and arcseconds.

appear to be hard enough not to have been selected as SSSs using the procedures applied to the *ROSAT* M31 survey data. Nevertheless, at least three of the sources with more than 20 counts would have likely been selected as *ROSAT* SSSs. Interestingly enough, it could be established that two of these three sources are transient by comparing the fluxes at these positions among different *Chandra* pointings or by studying data taken with *XMM-Newton*.

3. The bulge of M31 is rich in high-luminosity SSSs. By comparing among different *Chandra* pointings or by studying data taken with *XMM-Newton*, it has been found that 12 of 16 bulge sources are transient and that one additional source is highly variable.

The nondetection of four out of five *ROSAT*-discovered SSSs, combined with the failure to find any new sources with similarly soft X-ray spectra, appears to be puzzling for at least two reasons. First, if one assumes sources with constant brightness, could it be possible that the nondetection with *Chandra* is due to spurious detections with *ROSAT*? Second, if one assumes sources with variable X-ray emission, why do we not detect as many new sources with *Chandra* as we miss because they faded away between the *ROSAT* detection and the *Chandra* observation?

To answer these questions, we have embarked on a comprehensive reanalysis of the *ROSAT* data. In particular, in this paper we slightly revise the hardness ratio criterion used to select SSSs in the *ROSAT* Survey I data (§ 2), we analyze *ROSAT* PSPC Survey II (§ 4) and serendipitous PSPC observations (§ 5) for SSSs with the same criteria, and we present the first survey of *ROSAT* SSSs with *Chandra* (§ 3) and, for completeness, also include the public *XMM-Newton* observations (§ 6). We finally discuss the variability in § 7.

2. *ROSAT* PSPC SURVEY I

The search for SSSs in the M31 *ROSAT* data has been done so far only on the Survey I data. The hardness ratio criterion $HR1 + \sigma_{HR1} \leq -0.80$ [where HR1 is defined as the normalized count difference $(N_{50-200} - N_{10-40}) / (N_{10-40} + N_{50-200})$, with N_{a-b} denoting the number of counts in the PSPC between channels a and b (with the approximate conversion of channel/100 \approx energy in keV)] had been applied. A total of 15 sources were found (Greiner et al. 1996b; Supper et al.

1997). This hardness ratio criterion had been copied from a similar search done for the Magellanic Clouds and the whole PSPC all-sky survey. For those searches, contamination with cataclysmic binaries in the Magellanic Clouds or local F- and G-type stars (for the all-sky survey) was a problem that was mitigated by applying a very strict hardness ratio criterion. For M31, this problem does not exist, so it is worthwhile to reconsider the hardness ratio criterion for the Survey I data.

How much can we relax the hardness ratio criterion? Some SSSs may be hydrogen-burning WDs, and thus may reach effective temperatures of up to 70–80 eV. At a mean Galactic foreground absorbing column of 6×10^{20} cm⁻² (Dickey & Lockman 1990) and allowing for a similar M31 intrinsic absorption, this translates into a hardness ratio as low as HR1 \sim 0. On the other hand, supernova remnants can have hardness ratios as low as HR1 \sim -0.3, so we chose to avoid contamination by known source types. Therefore, we conservatively adapt HR1 = -0.5 as the new criterion, thus ensuring that no other class of sources is included.

The result of relaxing the hardness ratio criterion to $HR1 + \sigma_{HR1} \leq -0.5$ for selecting sources from the M31 *ROSAT* Survey I results in (only) seven additional sources (Table 1) with respect to the 15 sources obtained with the earlier selection of $HR1 + \sigma_{HR1} \leq -0.8$ (Greiner et al. 1996b; Supper et al. 1997). None of these seven new sources has a known long-wavelength (optical, infrared, or radio) counterpart, supporting our claim that these new sources have the same nature as the earlier selected 15 sources. This brings the number of “canonical” *ROSAT* SSSs to 22.

Kahabka (1999) has made a different selection, to also include possible SSSs that are located behind a substantial absorbing column. He applied the criteria $HR1 < +0.9$ and $HR1 + \sigma_{HR1} \leq -0.1$ and thereby selected 26 additional sources. This was motivated by the Galactic SSS RX J0925.7–4758 (Motch et al. 1994). However, eight of the 26 newly selected objects have been identified with foreground stars or supernova remnants (Kahabka 1999). Another source is likely a foreground cataclysmic variable. While Kahabka (1999) argues that the remaining sources are absorbed SSSs, there is also the possibility that they are of a nature similar to that of the already identified objects. We therefore did not include them in the present *Chandra* study, but only mention that we covered six objects of his sample with *Chandra*, two of which

TABLE 2
COUNT RATES OR UPPER LIMITS OF *ROSAT*-DETECTED SSSs AS SEEN WITH *Chandra* AND *XMM-Newton*

| NUMBER | NAME | <i>ROSAT</i> PSPC ^a | | | Chandra ACIS ^b | | | <i>XMM</i> pn ^c (counts ks ⁻¹) |
|---------|------------------------------|---|---|---|--|--|--|--|
| | | Survey I: 1991 Jul (counts ks ⁻¹) | Survey II: 1992–1993 (counts ks ⁻¹) | Serendipitous (counts ks ⁻¹) | Epoch 1: 2000 Nov 1–5 (counts ks ⁻¹) | Epoch 2: 2001 Mar 6–8 (counts ks ⁻¹) | Epoch 3: 2001 Jul 3 (counts ks ⁻¹) | |
| 1..... | RX J0037.4+4015 | 0.31 ± 0.31 | <0.40 | <1.15 | <0.99 ^d | ... | ... | ... |
| 2..... | RX J0038.5+4014 | 0.80 ± 0.28 | <0.13 | <2.84 | <0.41 | <0.35 | <0.54 | ... |
| 3..... | RX J0038.6+4020 | 1.73 ± 0.29 | 1.69 ± 0.35 | <2.66 | 0.95 ± 0.35 | 0.58 ± 0.14 | <0.29 | ... |
| 4..... | RX J0039.3+4047 | 0.26 ± 0.23 | <0.26 | ... | ... | ... | ... | ... |
| 5..... | RX J0039.6+4054 | 0.44 ± 0.44 | <0.49 | ... | ... | ... | ... | ... |
| 6..... | RX J0039.7+4030 | 2.03 ± 0.30 | 1.89 ± 0.34 | ... | ... | ... | ... | <1.28 (t) |
| 7..... | RX J0039.8+4053 | 1.07 ± 0.25 | <1.08 | ... | ... | ... | ... | ... |
| 8..... | RX J0040.4+4009 | 0.85 ± 0.32 | <0.20 | ... | ... | ... | ... | ... |
| 9..... | RX J0040.4+4013 | 0.50 ± 0.27 | <0.23 | ... | ... | ... | ... | ... |
| 10..... | RX J0040.7+4015 | 1.26 ± 0.32 | <0.42 | ... | ... | ... | ... | ... |
| 11..... | RX J0041.5+4040 | 0.32 ± 0.18 | <0.23 | ... | ... | ... | ... | ... |
| 12..... | RX J0041.8+4059 | 0.49 ± 0.24 | <0.47 | ... | <0.14 | <0.31 | <0.15 | <2.01 (t) |
| 13..... | RX J0042.4+4044 | 1.69 ± 0.32 | <0.32 | ... | ... | ... | ... | ... |
| 14..... | RX J0042.7+4107 | 1.04 ± 0.31 | <0.20 | ... | <3.47 ^d | ... | <3.49 ^d | <0.75 (m) |
| 15..... | RX J0043.5+4207 | 2.15 ± 0.55 | 2.20 ± 0.77 ^e | <2.07 | ... | ... | ... | ... |
| 16..... | RX J0044.0+4118 ^f | 2.46 ± 0.42 | <0.77 | <2.98 | ... | ... | ... | ... |
| 17..... | RX J0044.2+4117 | 0.95 ± 0.35 | <0.75 | <2.68 | ... | ... | ... | ... |
| 18..... | RX J0045.5+4206 | 3.14 ± 0.34 | 7.41 ± 0.66 | 3.96 ± 0.39 | ... | ... | ... | <7.59 (m) |
| 19..... | RX J0046.2+4144 | 2.15 ± 0.39 | <0.82 | 1.96 ± 0.34 | <1.22 | <0.79 | <0.14 | ... |
| 20..... | RX J0046.2+4138 | 1.12 ± 0.40 | <0.34 | <0.47 | <0.22 | <0.22 | <0.29 | ... |
| 21..... | RX J0047.4+4157 | <0.17 | 0.38 ± 0.15 | 0.60 ± 0.18 | ... | ... | ... | ... |
| 22..... | RX J0047.6+4159 | 1.23 ± 0.44 | <0.54 | 1.28 ± 0.25 | ... | ... | ... | ... |
| 23..... | RX J0047.6+4205 | 1.05 ± 0.36 | <0.17 | <0.32 | ... | ... | ... | ... |
| 24..... | RX J0047.8+4135 | <0.81 | 2.35 ± 0.80 | <0.76 | ... | <8.10 ^d | ... | ... |
| 25..... | RX J0045.4+4154 ^g | <0.22 | 2.77 ± 0.35 ^h | ... | <3.90 ^d | ... | <2.98 ^d | <0.51 (m) |

NOTES.—These count rates are on-axis rates as detected in each of the instruments (after correction for effective area), so they are not normalized. Conversion factors are given in footnotes b, c, and d. Sources 1–20, 22, and 23 are Survey I discoveries, sources 24 and 25 are Survey II discoveries, and source 21 was first found in a serendipitous observation.

^a Upper limits are at the 2 σ confidence level in the 0.1–0.4 keV band. The serendipitous pointings were done during 1993 January 2–30 for the sources in the first three rows and 1992 January 5–February for sources 15–24.

^b Upper limits are at the 2 σ confidence level in the 0.25–7 keV band. The conversion factor between the *ROSAT* PSPC and *Chandra* ACIS-S count rates (counts ks⁻¹) for these supersoft spectra ($kT \sim 40$ eV, $N_H = 6 \times 10^{20}$ cm⁻²) is 1:2; i.e., the ACIS-S count rate is twice the *ROSAT* PSPC rate. Sources not covered by the corresponding observation have blank entries.

^c The observation dates are different for each source: RX J0041.8+4059: 2002 January 12–13; RX J0045.4+4154 and RX J0045.5+4206: 2002 January 26–27; RX J0039.7+4030: 2002 January 24–25; RX J0042.7+4107: 2000 June 25, 2000 December 28 (upper limit is less than 2.98 counts ks⁻¹ [m]), 2001 June 29 (upper limit is less than 1.09 counts ks⁻¹ [m]). The code after the upper limits denotes the optical blocking filter used: t = thin, m = medium. The conversion factors between *ROSAT* PSPC and *XMM* EPIC pn count rates for SSSs (same parameters as in footnote b) are 1:6.7 for the thin filter and 1:5 for the medium filter.

^d These upper limits are for the FI CCD chips, for which the *ROSAT* PSPC–to–*Chandra* ACIS-I conversion factor is 1:0.2 only.

^e Detection at the 3 σ level; this source is not marked in Supper et al. (2001) as being detected in both surveys because of the 4 σ detection threshold.

^f Identified as a classical nova that erupted in September 1990; see Nedialkov et al. (2002).

^g This source was first reported by White et al. (1995), on the basis of *ROSAT* HRI observations, and seems to be a recurrent transient, as it also was detected in two *Chandra* HRC snapshot observations; Williams et al. (2004).

^h New estimate, which differs from that given in Supper et al. (2001).

are detected (the bright bulge source RX J0042.8+4115 and RX J0047.6+4132). For the four nondetections no statement about X-ray variability can be made, because of the harder spectra as compared to the canonical SSSs and the less favorable *ROSAT* PSPC–to–ACIS conversion rate (see below and Table 2).

3. CHANDRA OBSERVATIONS IN 2000/2001

Full details of the *Chandra* observations of M31 are given elsewhere (Paper I), so in addition to the results given in § 1, we repeat here only the few relevant points.

In order to cover the five *ROSAT* sources (2, 3, 12, 19, and 20) in each of the three different epochs, we arranged the pointing directions of the S3 chip such that the field of view rotated around the center of the S3 chip, and not the aim point

(see Fig. 1). As the field of view rotated from one epoch to the next, it also covered four other SSSs (1, 14, 24, and 25) with one of the FI chips (see footnote d in Table 2). Given that the *Chandra* S3 chip is a factor of 2 more sensitive than the *ROSAT* PSPC for SSSs (at $kT \sim 40$ eV and the low foreground absorption toward M31), each of the 15 ks observations was expected to provide of the order of 20–80 counts from each SSS.

Surprisingly, only one of the *ROSAT* sources (3) was detected during the *Chandra* observations (Paper I). Upper limits for the other sources were derived at the 2 σ confidence level using the full ACIS-S energy range (0.25–7 keV), since the background is dominated by the soft end of the spectrum anyway. The count rates for the detections and the upper limits are summarized in Table 2.

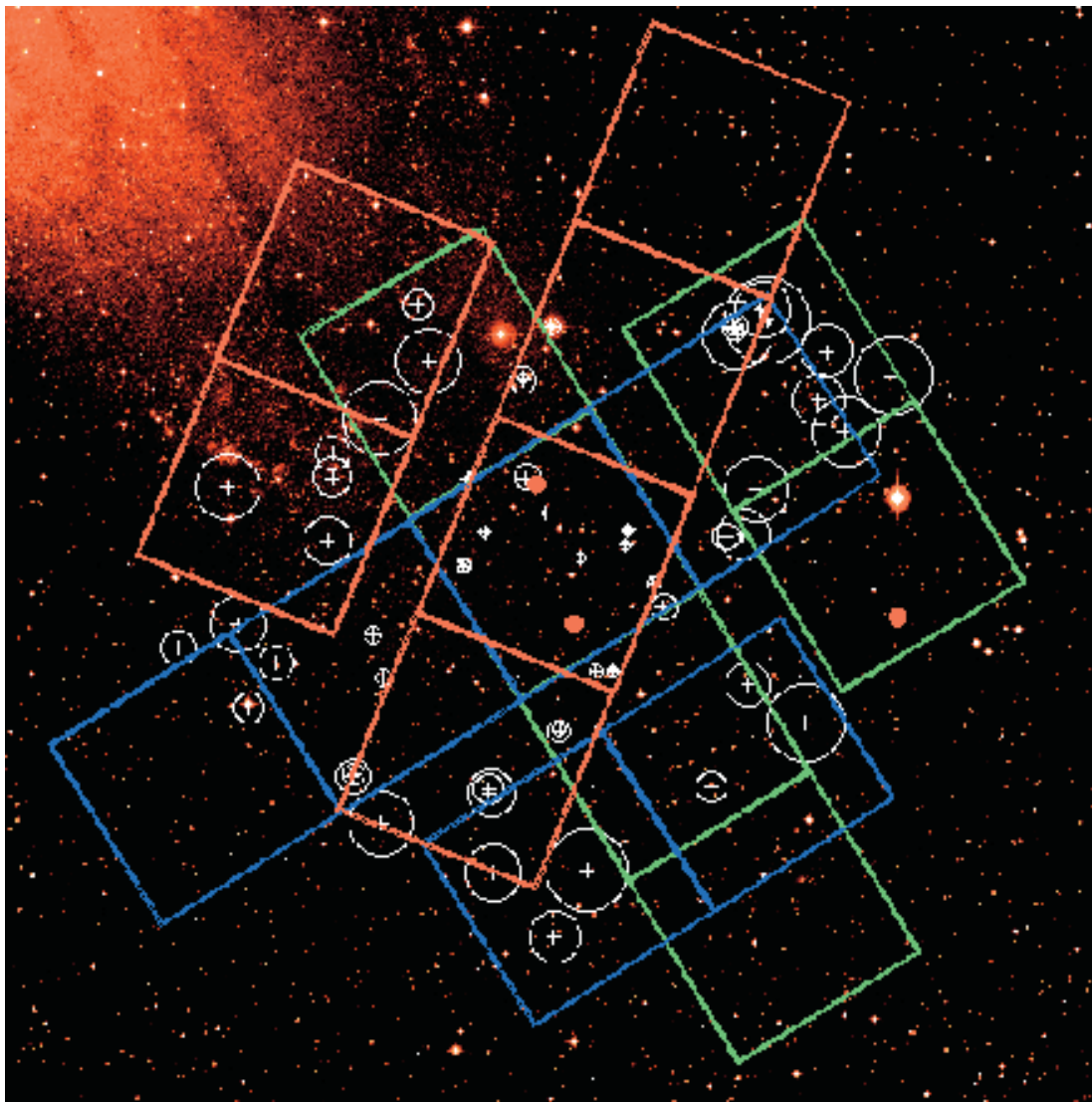


FIG. 1.—Optical image of the southern part of M31 covering one of the three *Chandra* fields, with the location of the six ACIS detectors overlaid for each of the three epochs (green, blue, and red for epochs 1–3, respectively). Note that the rotation of the field of view was arranged to happen around the center of the S3 chip, and not around the aim point. This leads to different off-axis angles for a given source during different epochs and explains why our upper limits in Table 2 are usually worse than the on-axis sensitivity of about 6×10^{-4} counts s^{-1} . Open white circles are for the detected sources, with the circle radii being proportional to the detected count rates. The three red filled dots denote the locations of three *ROSAT*-discovered SSSs (1, 2, and 3). The two of those located within the S3 chip (2 and 3) were covered in each of the three epochs, whereas the third (1) was only covered in the first. Only one of these *ROSAT* SSSs (3) has been detected with ACIS (open circle overlapping with one red dot), and this one only during the first two epochs. The pattern for the two other fields is similar.

4. *ROSAT* SURVEY II

4.1. *The Data*

The strong X-ray variability implied by the *Chandra* results motivated us to investigate the 22 canonical *ROSAT* SSSs in the second *ROSAT* PSPC survey. This second *ROSAT* survey was performed in 1992 July–August, 1993 January, and 1993 July–August and consisted of 96 different pointings of 2.5 ks each, offset from each other by about $10'$. After merging all these 96 individual pointings, the second PSPC survey provides a much higher spatial homogeneity, as compared to the six Survey I pointings of 25 ks each, and hence a higher sensitivity in the outer regions of the M31 disk. In addition, less area of M31 is lost in the second survey as a result of occultation by the PSPC window support structure, which is an important effect for the first survey. While the limiting sensitivity in the 0.1–2.0 keV range is 5×10^{-15} ergs cm^{-2} s^{-1}

in the first survey and 7×10^{-15} ergs cm^{-2} s^{-1} in the second survey, it is important to keep in mind the above differences, which lead to a substantially different spatial sensitivity pattern across the M31 disk between the two surveys.

A comparison of the source tables of the two surveys (Supper et al. 1997, 2001) shows that only three (3, 6, and 18) of the original $15 + 7 = 22$ *ROSAT* SSSs have also been detected in the second *ROSAT* survey. Furthermore, only one new SSS (24) has been discovered in the second *ROSAT* survey. In order to investigate this in more detail, we have used the merged data set of Supper et al. (2001) and reinvestigated the locations of the SSSs from the first survey by searching the map and maximum likelihood detection maps for SSSs at fainter levels than the 4σ list of Supper et al. (2001). We rediscover one source (15) at the 3σ level that had fallen below the 4σ threshold of the second survey. We also detect the White et al. (1995) transient (25), which had not been seen in

the first survey. With the one new SSS detection (24) and including the White et al. (1995) transient, this results in two new source detections in Survey II, and the sample of SSS in M31 increases to 24 sources (Table 2).

Finally, we derived upper limits for those sources that have not been detected. Upper limits have been determined by fitting a Gaussian profile with a width corresponding to the mean width of the point-spread function (PSF) of the merged pointings to the known positions, taking into account the vignetting and effective exposure time, and are given at the 2σ level in Table 2.

4.2. Understanding the Large Fraction of Nondetections

At first glance, this may cause doubts as to the quality of the data and/or analysis. However, we have been very careful in checking these causes and are convinced that these causes can be excluded. First, the original data analyses leading to the merged intensity and exposure maps of both surveys have been done by the same person with the same software less than one year apart (R. Supper in 1996–1997). Second, the majority of the hard X-ray sources are rediscovered, so if it were a technical problem, then the soft response would have to have suffered. Given the subsequent nondetections with *Chandra*, one would cast more doubts on the first survey than the second. However, there have been many observations of other soft sources after 1991, including noninteracting WDs and “monitoring” observations of soft sources for calibration purposes, which show that the soft response remained very stable until the end of the PSPC life.

The most likely effect leading to the nondetection of the Survey I sources is the “stretched” time sampling of the second survey, in conjunction with intrinsic X-ray variability of the SSSs. This survey was primarily done in three 2 month-long exposure epochs (in the following called EP1, EP2, and EP3), separated by 6 months each (between 1992 July and 1993 August). Typically, each of the 96 observations of 2.5 ks is spread over 2 days. However, for 13 out of the 96 pointings in the second survey, the exposure was split over two of these three epochs (either EP1–EP2 or EP2–EP3), and in two cases even over three epochs. The important fact to realize is that even when an observation was done within 2 days, it would not be sufficient to detect an SSS. Instead, at least two such observations are required for the brightest sources (6, 15, 16, and 18), and up to 15 observations for the faintest sources (1, 4, 5, and 11). Figure 2 shows the actual sampling for all SSSs and demonstrates that for most of these sources the Survey II exposure is spread over at least 3 weeks. In fact, only three sources are observed within one epoch (1 and 11 in EP1, 1992 July–August; and 24 in EP3, 1993 July–August), while nine sources are observed over two epochs and 12 even over all three epochs. Only if an SSS was constant over 6–8 months, i.e., over two epochs (either EP1–EP2 or EP2–EP3), or even 12 months (all three epochs) did it have a chance to be detected during the second *ROSAT* survey. If, on the contrary, the variability timescale of SSSs is shorter than 6 months but longer than 3 weeks, only a fraction of the total Survey II exposures would contribute to the potential detectability. From the detailed source coverage by the 96 individual pointings (Fig. 2), we determine that (1) 16 sources received enough exposure within a 3 week interval to be detectable at their Survey I count rates, out of which six have indeed been detected; (2) three sources (1, 4, and 5) were not detected because of insufficient exposure, if they remained constant, and (3) six sources (2, 8,

9, 10, 11, and 21) required the full survey exposure; of those, one source was detected.

5. SERENDIPITOUS *ROSAT* OBSERVATIONS

There have been three long (more than 15 ks) PSPC observations of M31 in the same time frame as Surveys I and II. While one of these (Observation ID [ObsID] 600245) does not cover any of our SSSs, the other two observations do cover three and nine SSSs. The former observation (ObsID 600244) was performed between 1993 January 2 and 30 for a total of 35.86 ks, the other (ObsID 600121) between 1992 January 5 and February 5 for a total of 44.73 ks. The latter observation is particularly interesting, because it happened before the second PSPC survey.

A source detection (within the EXSAS package; Zimmermann et al. 1994) was applied, including (1) a mask creation to screen all the parts of the image where the support structure of the PSPC entrance window affects the detectability of X-ray photons, (2) a map detection (“sliding window”) to find and remove all sources in order to (3) produce a background map with a bicubic spline fit to the resulting image. Finally, a maximum likelihood algorithm was applied to the data (e.g., Cruddace et al. 1988) in three separate PHA channel ranges. For the sources that are not detected, 2σ upper limits (Table 2) are computed in the 0.1–0.4 keV range, as described above.

None of the three sources covered by the 1993 January observation is detected. However, because of the large off-axis angles of these sources, the upper limits are all above the brightness of these sources during Survey I. That is, these upper limits are consistent with no variability.

For the other observation (ObsID 600121 in 1992), which covered nine SSSs, three are detected, in all cases at a level similar to the Survey I intensity. Since all these three sources are detected in the 1992 observation, i.e., about 6 months after the first and before the second PSPC survey, it reinforces the earlier interpretation that the SSSs found in the first PSPC survey are all real. The upper limits for another four sources are again high enough to be consistent with no variability, and two sources have faded (20 and 23).

Applying the revised hardness ratio criterion to these three pointed observations, and ignoring sources with bright (up to $V = 18$ mag) stars within their error box to avoid bright foreground stars (Greiner et al. 1996b), we find one new SSS (21 in Tables 1 and 2). This brings the total sample of *ROSAT* SSSs in M31 to 25.

6. *XMM-NEWTON* OBSERVATIONS

The bulge and disk of M31 were observed by *XMM-Newton* several times between 2000 and 2002. In particular, the central 15' area was observed four times (2000 June, 2000 December, 2001 June, and 2002 January; see Shirey et al. 2001; Osborne et al. 2001; Trudolyubov et al. 2002c), while four fields covering the northern and southern regions of the galaxy were visited by *XMM-Newton* in 2002 January (e.g., see Trudolyubov et al. 2002a). All data were taken with the three detectors (pn, MOS 1, and MOS 2) of the European Photon Imaging Camera (EPIC). The exposure time for the disk fields was about 60 ks each, while for the central region, the exposure time varied from 13 to 60 ks. The archival event lists were reprocessed and filtered with the *XMM-Newton* Science Analysis Software (XMMAS, ver. 5.4.1). We examined background flares of each observation and rejected intervals with high background level. Only data in the 0.2–12 keV range were used for the analysis.

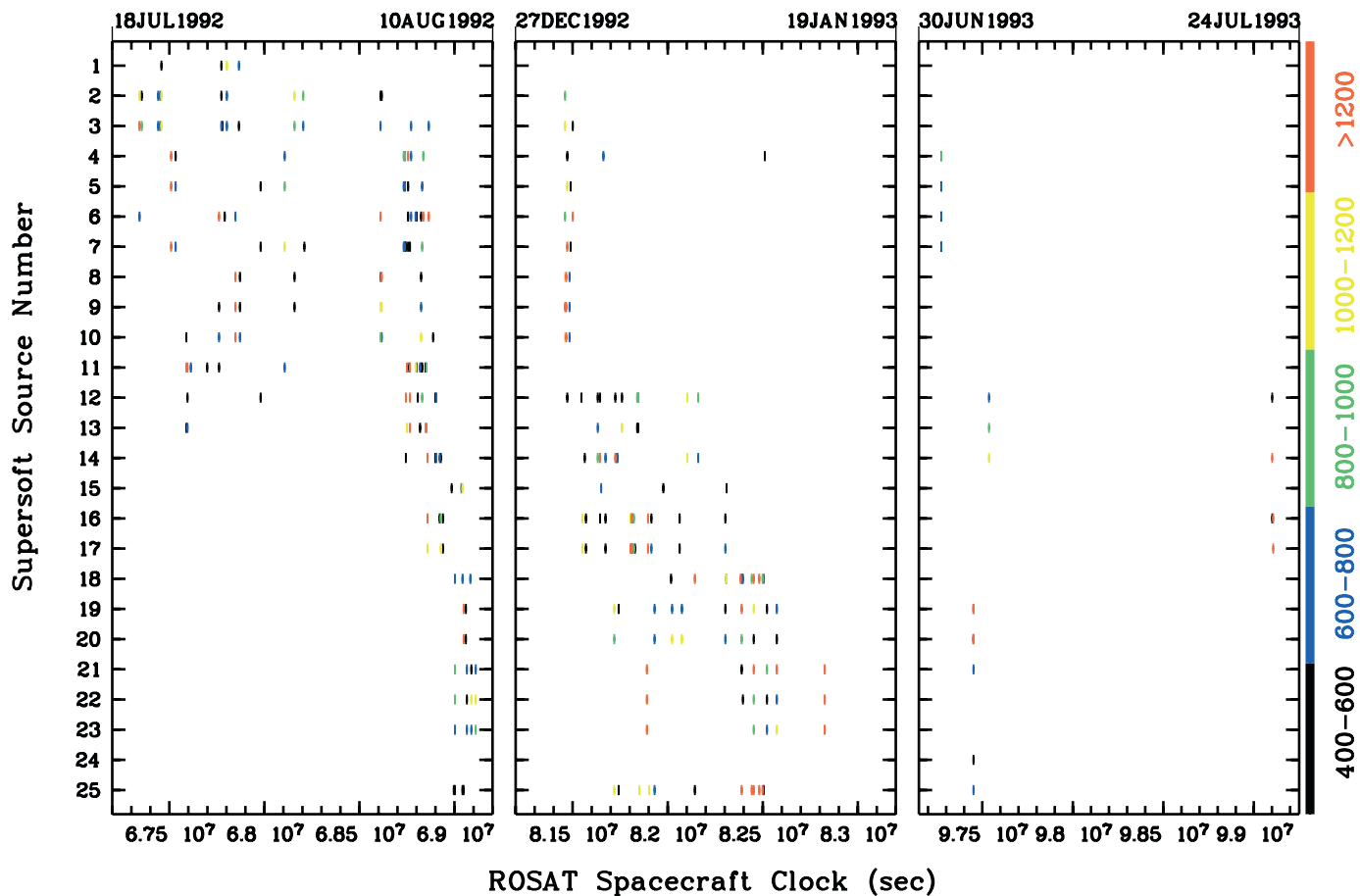


FIG. 2.—Temporal sequence of the individual observation intervals of M31 during the second *ROSAT* survey. This survey was conducted in two main observation epochs, namely, the southeastern part of M31 during 1992 July–August and the northwestern part during 1992 December–1993 January. For a few pointings, the exposures were completed only in 1993 June–July, marking a third observation epoch. Except for three sources (1, 11, and 24), the exposure spreads over more than one exposure epoch. Shown as color-coded dashes are the effective exposure times at the sky location of the 25 SSSs for all 96 individual pointed observations. The effective exposure has been computed by applying two factors to the on-axis, nominal exposure time: (1) the vignetting correction, i.e., the decrease of the effective area with off-axis angle, and (2) the square of the ratio of the radius of the PSF at the given off-axis angle to that on-axis (for 0.4 keV and 90% encircled energy), which is a correction for the decreasing source detection probability at larger off-axis angles due to the larger background area covered by the PSF. Effective exposure times below 400 s have been suppressed. The detection of an SSS with a brightness similar to that seen in the first *ROSAT* survey requires a minimum effective exposure of 4000 s for the brightest sources (6, 15, 16, and 18) and $\sim 40,000$ s for the faintest (1, 4, 5, and 11).

The (2σ) upper limits (Table 2) have been determined from the EPIC pn data by using the XMMSAS *emldetect* algorithm with an external source list and a maximum likelihood threshold of zero, thus providing upper limit counts derived from a fit of the three-dimensional PSF to the photon distribution.

No unbiased search for SSSs has been performed on the *XMM* data.

7. X-RAY VARIABILITY

7.1. The Results

Looking at Table 2, one can summarize the X-ray variability of the *ROSAT*-discovered SSSs in M31 as follows:

1. Combining the two *ROSAT* surveys, we find that out of the 22 SSSs detected during *ROSAT* Survey I, 18 sources were not detected during Survey II. Two new SSSs (24 and 25) were discovered relative to Survey I. From the four sources (4, 6, 15, and 18) detected in both surveys, three remained constant, while one was rising by a factor of 2. For eight of the sources (1, 4, 5, 7, 9, 11, 12, and 17), the upper limits during the full Survey II were consistent with the measured count rates during Survey I. Thus, about half of the SSSs (the above eight, plus

three sources that are seen in both surveys at similar count rates) were (or could have been) constant. In total, 10 sources (2, 8, 10, 13, 14, 16, 19, 20, 22, and 23) have faded by a factor of 2–5 on a timescale of 1 yr.

2. Three sources (18, 19, and 22) were detected in the serendipitous PSPC observation in 1992 January–February at intensities very similar to those measured 6 months earlier during the first PSPC survey. While one of these sources (18) increased in intensity thereafter, the other two (19 and 22) faded by a factor of 3–4 until the exposures of the second PSPC survey (6–12 months later).

3. The serendipitous PSPC observations provide upper limits for two sources (20 and 23), demonstrating that they faded by a factor of 3 within 6 months.

4. Including the *Chandra* and *XMM-Newton* observations, and thus the longer timescale of 9–12 yr, two of the constant sources (3 and 6) showed fading by a factor of 5–10, and two of the rising sources (24 and 25) faded by a factor of 5–25.

5. One of the *ROSAT*-discovered SSSs covered by *Chandra* observations (3) was “on” in the first and second sets of 15 ks *Chandra* observations but “off” in the third. Moreover, the count rate declined by nearly a factor of 2 between the two

Chandra epochs, and the decline between *ROSAT* Survey II and the first *Chandra* epoch was a factor of 3. This points to variability timescales of (shorter than) 3 months and a short duty cycle. In fact, this source could be similar to the fading source RX J0527.8–6954 (Greiner et al. 1996a).

6. The *Chandra* observations do not reveal any new SSSs with a hardness ratio and count rate comparable to those of the *ROSAT*-discovered sources (>20 counts in 15 ks), but *Chandra*'s spatial coverage was only 5% of the M31 disk.

In conclusion, when sorting for variability timescale and considering only variability with an amplitude larger than a factor of 2, we have

1. one source (3) that varied over a timescale of 3 months,
2. seven sources (18–24) that varied over a timescale of 6 months,
3. seven sources (2, 8, 10, 13, 14, 16, and 25) that varied over a timescale of 1 yr,
4. two sources (6 and 12) that varied over a timescale of more than 5 yr, and
5. eight sources (1, 4, 5, 7, 9, 11, 15, and 17) for which no statement about variability can be made.

7.2. Possible Origin of the X-Ray Variability

If the majority of these sources are CBSSs, one possible explanation for this rapid variability could be photospheric expansion and contraction of the WD envelope, which can shift the radiation out of and then back into the X-ray regime. This is the mechanism suspected to be responsible for the X-ray variability in RX J0513.9–6951 (Reinsch et al. 1996, 2000) and CAL 83 (Greiner & Di Stefano 2002). The interesting point, however, is that if this were true, about half of these sources (just considering sources with a variability timescale shorter than 1 yr) would operate at rather high mass transfer rates, corresponding to the upper limit of the stable H-burning regime. One then may ask where to find the sources with mass transfer rates within the stable burning region. Whether this is an observational bias (since we preferentially detect the high-temperature, high-luminosity sources in M31, for sensitivity reasons) or can be accommodated in population synthesis models remains to be evaluated in more detail.

However, we do not know whether all the SSSs in M31 are CBSSs. There are several other alternatives that also would explain variability: (1) Postnova SSSs should (and have been observed to) dim over time. The number of SSSs that can be postnovae is constrained by independent estimates of the nova rate. (2) Pre-WDs can reignite (the “born again” phenomenon); this happens over timescales short enough that the associated planetary nebulae should still be visible. (3) Supersoft binaries that are neutron stars sometimes exhibit low/hard states. One possible example, though not conclusively identified as a neutron star, is 1E 1339.8+2837, which switches between high/soft and low/hard states (Dotani et al. 1999). (4) Soft X-ray emission is very vulnerable to column densities above a few times 10^{20} cm $^{-2}$, so variable absorption due, e.g., to variable mass loss is a possible cause of variability.

7.3. The Fraction of Novae and Recurrent Novae

It is interesting to note that one of the faders (RX J0044.0+4118, source 16) has been optically identified as a classical nova that erupted in 1990 (Nedialkov et al. 2002). Thus, one could speculate whether the above difference in the numbers of faders and risers is due to a fraction of classical novae.

However, observing at a given time (i.e., 1991 or 2000) should show a similar number of novae being on in their soft X-ray state, unless the supersoft phase of novae is so short and/or rare that catching one nova during *ROSAT* Survey I was a unique chance coincidence. Indeed, a survey of the X-ray emission of local and nearby novae has shown that only 3 out of 108 novae have revealed a supersoft phase (Orio et al. 2001). While two more supersoft novae have been identified in the meantime, the majority have rather short supersoft phases, of the order of weeks to a few months. This line of reasoning would then imply that on statistical grounds, RX J0044.0+4118 is most likely the only nova in the sample of the *ROSAT*-discovered M31 SSSs. Thus, we do not think that classical novae can change the ratio of faders to risers or that they comprise a substantial fraction of the *ROSAT*-discovered M31 SSSs.

A similar result is obtained when considering the total nova rate of ~ 37 novae yr $^{-1}$ per M31 disk (Shafter & Irby 2001). Since *ROSAT* Survey I was done in about 1 month and the duration of the supersoft phase in novae is of a similar short timescale (e.g., Greiner et al. 2003), at maximum two of the *ROSAT*-discovered M31 SSSs should be novae, even if all novae undergo a supersoft phase.

The outburst rate of recurrent novae in M31 has been estimated to be only 10% of the rate of classical novae (Della Valle & Livio 1996). While this may be an underestimate due to the lower luminosity of recurrent novae and the possible lack of sensitivity to part of the population, it is clear that recurrent novae cannot explain the frequency of SSS variability in M31.

8. CONCLUSIONS

The evidence from *ROSAT*, *Chandra*, and *XMM* is that SSSs tend to be highly variable, perhaps more variable than any other class of X-ray binary, most notably the hard sources comprising a substantial number of X-ray binaries (Trudolyubov et al. 2002a). A large fraction (30%) of SSSs are transients, with turnoff or turnon times on the order of a few months. The majority of the sources that have fallen below detectability limits have not been detected again. This may argue that the duty cycle is low, while activity times are on the order of months or years. With an on-time duration of months and a duty cycle of, e.g., 40%, we have only a 10% chance of detecting a source that was “on” during one observation in a second uncorrelated observation and a 16% chance of detecting any given SSS in two unrelated observations, consistent with our finding.

In addition, the spatial coverage of M31 with *Chandra* was small (less than 5%), since the coverage for SSS by *Chandra* is primarily given by the S3 chip. Thus, the likelihood of detecting new SSSs with *Chandra* was small. Population studies have estimated the total SSS population in M31 to be ~ 1000 (Di Stefano & Rappaport 1994). With an assumed duty cycle of 10%, this would correspond to a density of active SSSs of 3×10^{-3} arcmin $^{-2}$, or 0.02 per S3 chip.

While it is unlikely that novae are responsible for the strong X-ray variability in SSS, its physical cause remains to be explained. Both better sampling of the light curve and optical identifications and subsequent optical monitoring seem to be required to deduce insight into the variability mechanism(s).

We finally note that the more frequent *Chandra* and *XMM* observations over the last three years have revealed a number of supersoft X-ray transients (e.g., Shirey 2001; Trudolyubov et al. 2002b). While their nature remains to be established as well, they support the notion of the strong variability of SSSs.

J. G. is particularly grateful to Rodrigo Supper for providing the merged *ROSAT* PSPC data of the two M31 surveys, which alone allowed the derivation of the upper limits presented

here. R. D. acknowledges support by NASA/*Chandra* grant GO1-2022X, LTSA grant NAG5-10705, and the Croucher Foundation.

REFERENCES

- Cruddace, R. G., Hasinger, G. R., & Schmitt, J. H. M. M. 1988, in *Astronomy from Large Databases*, ed. F. Murtagh F. & A. Heck (Garching: ESO), 177
- Della Valle, M., & Livio, M. 1996, *ApJ*, 473, 240
- Dickey, J. M., & Lockman, F. J. 1990, *ARA&A*, 28, 215
- Di Stefano, R., & Rappaport, S. 1994, *ApJ*, 437, 733
- Di Stefano, R., et al. 2004, *ApJ*, 610, 247 (Paper I)
- Dotani, T., Asai, K., & Greiner, J. 1999, *PASJ*, 51, 519
- Greiner, J. 2000, *NewA*, 5, 137
- Greiner, J., & Di Stefano, R. 2002, *A&A*, 387, 944
- Greiner, J., Orio, M., & Schartel, N. 2003, *A&A*, 405, 703
- Greiner, J., Schwarz, R., Hasinger, G., & Orio, M. 1996a, *A&A*, 312, 88
- Greiner, J., Supper, R., & Magnier, E. A. 1996b, in *Supersoft X-Ray Sources*, ed. J. Greiner (LNP 472; Berlin: Springer), 75
- Kahabka, P. 1999, *A&A*, 344, 459
- Long, K. S., Helfand, D. J., & Grabelsky, D. A. 1981, *ApJ*, 248, 925
- Motch, C., Hasinger, G., & Pietsch, W. 1994, *A&A*, 284, 827
- Nedialkov, P. L., Orio, M., Birkle, K., Conselice, C., Della Valle, M., Greiner, J., Magnier, E., & Tikhonov, N. A. 2002, *A&A*, 389, 439
- Orio, M., Covington, J., & Ögelman, H. 2001, *A&A*, 373, 542
- Osborne, J. P., et al. 2001, *A&A*, 378, 800
- Reinsch, K., van Teeseling, A., Beuermann, K., & Abbott, T. M. C. 1996, *A&A*, 309, L11
- Reinsch, K., van Teeseling, A., King, A. R., & Beuermann, K. 2000, *A&A*, 354, L37
- Shafter, A. W., & Irby, B. K. 2001, *ApJ*, 563, 749
- Shirey, R. 2001, *IAU Circ.*, 7659, 1
- Shirey, R., et al. 2001, *A&A*, 365, L195
- Supper, R., Hasinger, G., Lewin, W. H. G., Magnier, E. A., van Paradijs, J., Pietsch, W., Read, A. M., & Trümper, J. 2001, *A&A*, 373, 63
- Supper, R., Hasinger, G., Pietsch, W., Trümper, J., Jain, A., Magnier, E. A., Lewin, W. H. G., & van Paradijs, J. 1997, *A&A*, 317, 328
- Trudolyubov, S. P., Borozdin, K. N., Priedhorsky, W. C., Mason, K. O., & Cordova, F. A. 2002a, *ApJ*, 571, L17
- . 2002b, *IAU Circ.*, 7798, 2
- Trudolyubov, S. P., Borozdin, K. N., Priedhorsky, W. C., Osborne, J. P., Watson, M. G., Mason, K. O., & Cordova, F. A. 2002c, *ApJ*, 581, L27
- van den Heuvel, E. P. J., Bhattacharya, D., Nomoto, K., & Rappaport, S. A. 1992, *A&A*, 262, 97
- White, N. E., Giommi, P., Heise, J., Angelini, L., & Fantasia, S. 1995, *ApJ*, 445, L125
- Williams, B. F., Garcia, M. R., Kong, A. K. H., Primini, F. A., King, A. R., Di Stefano, R., & Murray, S. S. 2004, *ApJ*, 609, 735
- Zimmermann, H.-U., Becker, W., Belloni, T., Döbereiner, S., Izzo, C., Kahabka, P., & Schwendtker, O. 1994, *EXSAS User's Guide* (4th ed.; MPE Rep. 257; Garching: MPE)